

EJECTA–CIRCUMSTELLAR MEDIUM INTERACTION IN HIGH-DENSITY ENVIRONMENT CONTRIBUTION TO KILONOVA EMISSION: APPLICATION TO GRB 191019A

SUO-NING WANG¹, HOU-JUN LÜ¹, YONG YUAN², HAO-YU YUAN³, JARED RICE⁴, MENG-HUA CHEN¹, AND EN-WEI LIANG¹
Draft version February 21, 2024

ABSTRACT

The nearby long-duration GRB 191019A recently detected by Swift lacks an associated supernova and belongs to a host galaxy with little star formation activity, suggesting that the origin of this burst is the result of a merger of two compact objects with dynamical interactions in a high-density medium of an active galactic nucleus. Given the potential motivation of this event, and given that it occurs in such a high-density environment, the ejecta-circumstellar medium (CSM) interaction cannot be ignored as possibly contributing to the kilonova emission. Here, we theoretically calculate the kilonova emission by considering the contribution of the ejecta-CSM interaction in a high-density environment. We find that the contribution to the kilonova emission from the ejecta-CSM interaction will dominate at a later time, and a smaller ejecta mass will have a stronger kilonova emission from the ejecta-CSM interaction. Moreover, we try to apply it to GRB 191019A, but we find that it is difficult to identify the possible kilonova emission from the observations, due to the contribution of the bright host galaxy. On the other hand, less injected mass (less than $M_{\text{ej}} = 2 \times 10^{-5} M_{\odot}$) will be required if one can detect the kilonova emission associated with a GRB 191019A-like event in the future. The r -process-powered and spin energy contributions from the magnetar are also discussed.

Subject headings: Gamma-ray burst: general

1. INTRODUCTION

Merger of two compact stars, such as neutron star–neutron star (NS-NS) mergers (Paczynski 1986; Eichler et al. 1989) or neutron star–black hole (NS-BH) mergers (Paczynski 1991), are thought to be potential sources of gravitational-wave (GW) radiation, short-duration gamma-ray bursts (GRBs), as well as optical/infrared transients (called kilonovae; Berger 2014; Zhang 2018). The first “smoking gun” evidence to support this hypothesis was the direct detection of a GW event (GW170817) by Advanced LIGO and Virgo that was associated with the short GRB 170817A and kilonova AT2017gfo (Abbott et al. 2017; Covino et al. 2017; Evans et al. 2017; Goldstein et al. 2017; Kasen et al. 2017; Savchenko et al. 2017; Zhang et al. 2018).

Phenomenally, GRBs are divided into those of long and short durations, with a division line at the observed duration $T_{90} \sim 2$ s (Kouveliotou et al. 1993), and it has been suggested that they are likely related to compact star merger and the deaths of massive stars, respectively (Zhang 2018). However, the duration of a GRB is energy- and instrument-dependent (Qin et al. 2013), suggesting that it may not be directly related to the progenitors of GRBs (Lü et al. 2010, 2014). It requires a

multiple observational criteria to judge the progenitors of GRBs (Zhang et al. 2009). A small fraction of short-duration GRBs were reported to be associated with kilonova candidates before the discovery of GW 170817/GRB 170817A/AT2017gfo (see Metzger 2019 for a review)—for example, GRB 130603B (Berger et al. 2013; Tanvir et al. 2013), GRBs 050709 and 070809 (Jin et al. 2016, 2020), GRB 080503 (Metzger & Piro 2014; Gao et al. 2015), and GRB 160821B (Lü et al. 2017; Lamb et al. 2019; Troja et al. 2019). On the other hand, excepting the above short-duration GRBs, several nearby short-duration GRBs with extended emission (EE) lacking an associated supernova but containing a possible kilonova signature were claimed to be from compact star mergers—for example, GRB 060614 (Della Valle et al. 2006; Fynbo et al. 2006; Gal-Yam et al. 2006; Gehrels et al. 2006; Yang et al. 2015), GRB 211211A (Rastinejad et al. 2022; Troja et al. 2022; Yang et al. 2022; Chang et al. 2023; Gompertz et al. 2023), and GRB 211227A (Lü et al. 2022; Ferro et al. 2023).

Recently, a nearby peculiar long-duration GRB 191019A without EE emission that triggered the Swift Burst Alert Telescope (BAT; Simpson et al. 2019) with redshift $z = 0.248$ (Levan et al. 2023) has generated excitement. More interestingly, no associated supernova signature was detected for GRB 191019A and the host galaxy has no significant star formation activity (Levan et al. 2023). This suggests that the origin of GRB 191019A is unlikely to be the death of a massive star (Levan et al. 2023), but that dynamical interactions in the dense nucleus of the host via compact object merg-

¹Guangxi Key Laboratory for Relativistic Astrophysics, School of Physical Science and Technology, Guangxi University, Nanning 530004, China; lhj@gxu.edu.cn

²School of Physics Science And Technology, Wuhan University, No.299 Bayi Road, 430072, Wuhan, Hubei, China

³School of Physics, Huazhong University of Science and Technology, Wuhan 430074, China

⁴Department of Mathematics and Physical Science, Southwestern Adventist University, Keene, TX 76059, USA

ers could naturally explain the observations (Levan et al. 2023). For example, gas drag (Tagawa et al. 2020) and the clustering of compact objects in migration traps promote binary formation through dynamic interactions (Bellovary et al. 2016; McKernan et al. 2020). Lazzati et al. (2023) proposed that the GRB 191019A originated in a binary compact merger with an intrinsic prompt emission duration of ~ 1.1 s, which is stretched in time by the interaction with a high-density external medium $\sim 10^7\text{--}10^8\text{ cm}^{-3}$ (Lazzati et al. 2022). If this is the case, a kilonova emission associated with GRB 191019A should be powered after the merger of the compact stars, and the contribution of an ejecta–circumstellar medium (CSM) interaction producing a kilonova cannot be ignored in such a dense external medium (Qi et al. 2022; Ren et al. 2022). In previous studies, the ejecta–CSM interaction has been invoked to interpret the observations of some superluminous supernovae (Chevalier & Fransson 1994; Smith & McCray 2007; Chevalier & Irwin 2011; Chatzopoulos et al. 2012, 2013; Nicholl et al. 2014; Wang et al. 2016; Liu et al. 2018), but never has been used to interpret any kilonova emission associated with short GRBs.

From a theoretical point of view, the kilonova emission from a merger of two compact stars is generated by the ejected materials, powered by radioactive decay from the r -process, and is nearly isotropic (Li & Paczyński 1998; Metzger et al. 2010; Berger 2011; Rezzolla et al. 2011; Hotokezaka et al. 2013; Rosswog et al. 2013; Jin et al. 2015). On the other hand, the magnetar central engine can be formed as the remnant, depending on the mass of the nascent NS, if the merger of the two compact stars is NS-NS or an NS and a white dwarf (NS-WD) (Usov 1992; Dai & Lu 1998; Zhang & Mészáros 2001; Dai et al. 2006; Rowlinson et al. 2010). If this is the case, the spin energy of the magnetar can be comparable to or even larger than the radioactive decay energy and may power a brighter kilonova (called a “merger-nova”; Yu et al. 2013; Zhang 2013; Metzger & Piro 2014; Gao et al. 2017; Lü et al. 2017), such as 160821B (Lü et al. 2017) and GRB 170817A (Yu et al. 2018). It is also possible that the magnetic wind from the accretion disk of a newborn BH could heat up the neutron-rich merger ejecta and provide additional energy to the transients if the central engine is a BH for NS-BH or NS-NS mergers (Yang et al. 2015; Ma et al. 2021; Yuan et al. 2021), such as GRB 160821B (Ma et al. 2021; Yuan et al. 2021).

If the merger of two compact stars is indeed operating in GRB 191019A, then a question arises: how bright is the kilonova emission associated with GRB 191019A when we simultaneously consider the different types of energy sources, i.e. r -process-powered, spin energy from a magnetar, and the contribution from an ejecta–CSM interaction? This paper aims to address this interesting question through detailed calculations of the kilonova emission, which are then compared with the calculated results for the kilonova from the observational data of GRB 191019A. This paper is organized as follows. The models of the kilonova energy sources we use are shown in Section 2, and Section 3 presents the basic observations of GRB 191019A. In Section 4, we show the results of the kilonova calculations to compare with the observational data of GRB 191019A. Conclusions are drawn in Section 5 with some additional discussions. Through-

out the paper, we use the notation $Q_n = Q/10^n$ in CGS units, which means that Q_n is the unit of 10^n (such as $E_{52} = E/(10^{52}\text{ erg})$). We adopt a concordance cosmology with parameters $H_0 = 71\text{ km s}^{-1}\text{ Mpc}^{-1}$, $\Omega_M = 0.30$, and $\Omega_\Lambda = 0.70$.

2. BASIC MODEL OF KILONOVA ENERGY SOURCES

2.1. r -process nucleosynthesis

The ejecta from NS-NS or NS-BH mergers carries a large amount of free neutrons. The ejecta expands in space at a nearly constant speed and the neutron capture time scale is shorter than the β -decay time scale in such a dense neutron-rich environment. This allows the rapid neutron capture process (called r -process) to quickly synthesize elements heavier than Fe. The heavier elements are unstable and heat the ejecta through radioactive decay. Photons are trapped in the ejecta, but are eventually released from the photosphere to power the kilonova, which radiates in the ultraviolet, optical, and infrared bands (Li & Paczyński 1998; Metzger et al. 2010; Metzger 2017).

The total energy of the ejecta can be written as $E_{\text{ej}} = (\Gamma - 1)M_{\text{ej}}c^2 + \Gamma E'_{\text{int}}$, where E'_{int} is the internal energy measured in the comoving frame, M_{ej} is the ejecta mass, c is the speed of light, and Γ is the Lorentz factor. Based on energy conservation, one has

$$dE_{\text{ej}} = (L_{\text{inj}} - L_e)dt, \quad (1)$$

where L_e and L_{inj} are the radiated bolometric luminosity and the injection luminosity, respectively. Within the r -process scenario, the injection luminosity is contributed to by radioactive power (L_{ra}):

$$L_{\text{inj}} = L_{\text{ra}}. \quad (2)$$

The radioactive power in the comoving frame can be defined as

$$\begin{aligned} L'_{\text{ra}} &= \frac{L_{\text{ra}}}{\mathcal{D}^2} \\ &= 4 \times 10^{49} M_{\text{ej},-2} \times \left[\frac{1}{2} - \frac{1}{\pi} \arctan \left(\frac{t' - t'_0}{t'_\sigma} \right) \right]^{1.3} \text{ erg s}^{-1}, \end{aligned} \quad (3)$$

where $t'_0 \sim 1.3$ s and $t'_\sigma \sim 0.11$ (Korobkin et al. 2012), and $\mathcal{D} = 1/[\Gamma(1 - \beta)]$ is the Doppler factor with $\beta = \sqrt{1 - \Gamma^{-2}}$. The comoving time dt' can be connected with the observer’s time via $dt' = \mathcal{D}dt$.

Together with the above considerations, the equation for the dynamic evolution of the ejecta can be expressed as

$$\frac{d\Gamma}{dt} = \frac{L_{\text{inj}} - L_e - \Gamma \mathcal{D} (dE'_{\text{int}}/dt')}{M_{\text{ej}}c^2 + E'_{\text{int}}}. \quad (4)$$

The evolution of internal energy in the comoving frame can be written as (Kasen & Bildsten 2010; Yu et al. 2013)

$$\frac{dE'_{\text{int}}}{dt'} = L'_{\text{inj}} - L'_e - \mathcal{P}' \frac{dV'}{dt'}. \quad (5)$$

The pressure $\mathcal{P}' = E'_{\text{int}}/3V'$ is dominated by radiation, and the evolution of the comoving volume can be written as

$$\frac{dV'}{dt} = 4\pi R^2 \beta c, \quad (6)$$

where R is the radius of the ejecta and β is the velocity of the kilonova ejecta, which is equal to v_{KN} . One has

$$\frac{dR}{dt} = \frac{\beta c}{(1 - \beta)} \quad (7)$$

such that the radiated bolometric luminosity in the co-moving frame can be expressed as (Kasen & Bildsten 2010; Kotera et al. 2013)

$$L'_e = \begin{cases} \frac{E'_{\text{int}} c}{\tau R/\Gamma}, & t \leq t_\tau \\ \frac{E'_{\text{int}} c}{R/\Gamma}, & t > t_\tau \end{cases}, \quad (8)$$

where $\tau = \kappa(M_{\text{ej}}/V')(R/\Gamma)$ is the optical depth of the ejecta, κ is the opacity, and t_τ is the time at $\tau = 1$.

The radiation of the ejecta comes from the photosphere R_{ph} with a blackbody radiation spectrum. The effective temperature can be defined as (Yu et al. 2018)

$$T_e = \left(\frac{L_e}{4\pi R_{\text{ph}}^2 \sigma_{\text{SB}}} \right)^{1/4}, \quad (9)$$

where σ_{SB} is the Stephan–Boltzman constant. The observed flux density at frequency ν can be calculated as

$$F_\nu^{\text{ejcta}} = \frac{2\pi h \nu^3 R^2}{D_L^2 c^2} \frac{1}{\exp(h\nu/kT_e) - 1}, \quad (10)$$

where h is the Planck constant and D_L is the luminosity distance of the source.

2.2. Spindown energy

For a stable NS with an initial spin period P_i , the total rotational energy is $E_{\text{rot}} \sim 2 \times 10^{52} I_{45} M_{1.4} R_6^2 P_{i,-3}^{-2}$ erg, where M , R , and I are the mass, radius, and moment of inertia of the NS, respectively. The spindown luminosity of a stable NS as a function of time can be expressed by the magnetic dipole radiation formula equation (Zhang & Mészáros 2001; Lü et al. 2018):

$$L_{\text{sd}} = L_0 \left(1 + \frac{t}{t_{\text{sd}}} \right)^\alpha \quad (11)$$

where $L_0 \simeq 1.0 \times 10^{47}$ erg s $^{-1}$ ($B_{p,14}^2 P_{i,-3}^{-4} R_6^6$), and $t_{\text{sd}} \simeq 2 \times 10^5$ s ($I_{45} B_{p,14}^{-2} P_{0,-3}^2 R_6^{-6}$) are the characteristic spindown luminosity and timescale, respectively. t is the time in the observed frame and α is equal to -1 and -2 when the energy loss is dominated by GW radiation (Lasky & Glampedakis 2016; Lü et al. 2020) and magnetic dipole radiation (Zhang & Mészáros 2001), respectively. Sometimes, α may be less than -2 , which corresponds to the situation of a supermassive NS central engine collapsing into a BH (Rowlinson et al. 2010; Yuan et al. 2021).

If the central engine of a short GRB is a stable NS, the main power source of the kilonova should no longer be limited to the r -process and the spin energy of the NS may be comparable to or even larger than the radioactive decay energy. In this case, the ejection luminosity should have contributions from both the spindown luminosity (L_{sd}) and radioactive power (L_{ra}):

$$L_{\text{inj}} = \xi L_{\text{sd}} + L_{\text{ra}}, \quad (12)$$

where ξ corresponds to the converted efficiencies (fixed to 0.3) from spindown luminosity to radiation (Zhang & Yan 2011). The subsequent operations are the same as in the previous part.

2.3. Ejecta–CSM interaction

If the external medium of a short GRB is dense enough, we have to consider the contribution of an ejecta–CSM interaction to the kilonova emission. The ejecta–CSM interaction model involving multiple shells/winds has been invoked to interpret supernova light curves with multiple peaks (Wang et al. 2016; Liu et al. 2018). Following the same method of ejecta–CSM interaction that has been used in supernova explosions, we invoke the ejecta–CSM interaction model involving one shell to calculate the kilonova emission. In this section, we will present the details of this ejecta–CSM interaction model.

The ejecta interacting with the pre-existing CSM can result in two shocks: a forward shock (FS) that propagates through the CSM and a reverse shock (RS) that sweeps up the kilonova ejecta. Based on numerical simulations of supernova explosions, the density of the supernova ejecta is a power-law distribution (Chevalier 1982; Chevalier & Fransson 1994; Liu et al. 2018). We assume that the density distribution of the kilonova ejecta also obeys a power-law distribution (Matzner & McKee 1999). Thus, the density profile of the outer part of the kilonova ejecta is written as

$$\rho_{\text{out}} = g_n t^{n-3} r^{-n}, \quad (13)$$

where n is the power-law index of the outer part of the ejecta that depends on the kilonova progenitor star. g_n is the scaling parameter of the density profile, and it is given by (Chevalier & Fransson 1994; Chatzopoulos et al. 2012)

$$g_n = \frac{1}{4\pi(n-\delta)} \frac{[2(5-\delta)(n-5)E_{\text{KN}}]^{(n-3)/2}}{[(3-\delta)(n-3)M_{\text{ej}}]^{(n-5)/2}}, \quad (14)$$

where δ is the power-law index of the inner density profile and E_{KN} is the total kilonova energy. The density of a circumstellar shell is written as

$$\rho_{\text{CSM}} = q r^{-s}, \quad (15)$$

where q is a scaling constant and s is the power-law index for a CSM density profile. $s = 0$ represents a uniform-density shell. Here, we adopt a uniform-density shell ($s = 0$) to do the calculations and obtain the density of the ambient material $\rho_{\text{CSM}} = q$. Moreover, in order to test how sensitive the kilonova emission is for n , we calculate the kilonova emission that is contributed from the ejecta–CSM interaction with varying n . We find that a smaller-quality n is corresponding to a longer time and brighter emission from the CSM interaction. The kilonova emission from the ejecta–CSM interaction with $n = 7$ is comparable with observations, so we adopt $n = 7$ to do the calculations.

A contact discontinuity separates the shocked CSM and the shocked ejecta. Its radius (R_{cd}) can be described by the self-similar solution (Chevalier 1982)

$$R_{\text{cd}} = \left(\frac{A g_n}{q} \right)^{\frac{1}{n-s}} t^{\frac{(n-3)}{(n-s)}}, \quad (16)$$

where A is a constant. The radii of the FS and RS are written as

$$R_{\text{FS}}(t) = R_{\text{in}} + \beta_{\text{FS}} R_{\text{cd}} \quad (17)$$

and

$$R_{\text{RS}}(t) = R_{\text{in}} + \beta_{\text{RS}} R_{\text{cd}}, \quad (18)$$

where R_{in} is the initial radius of the interaction. β_{FS} and β_{RS} are constants representing the ratio of the shock radius to the contact discontinuity radius, respectively. The values of β_{FS} and β_{RS} are shown in Table 1 of Chevalier (1982). The self-similar solutions for the structure of the interaction region require to $n > 5$. Based on the result in Liu et al. (2018), we adopt $n = 7$, which is used in the outer part of type I supernovae. Given $n = 7$ and $s = 0$, one has $\beta_{\text{FS}} = 1.181$, $\beta_{\text{RS}} = 0.935$, and $A = 1.2$. The ejecta–CSM interaction will convert the kinetic energy to radiation. The input luminosity function of the FS is (Chatzopoulos et al. 2012)

$$L_{\text{FS}}(t) = \frac{2\pi}{(n-s)^3} g_n^{\frac{5-s}{n-s}} q^{\frac{n-5}{n-s}} (n-3)^2 (n-5) \beta_{\text{FS}}^{5-s} A^{\frac{n-5}{n-s}} \times (t + t_{\text{int}})^{\alpha_i} \theta(t_{\text{FS,BO}} - t), \quad (19)$$

and for the RS it is (Wang et al. 2016)

$$L_{\text{RS}}(t) = 2\pi \left(\frac{Ag_n}{q} \right)^{\frac{5-n}{n-s}} \beta_{\text{RS}}^{5-n} g_n \left(\frac{n-5}{n-3} \right) \times \left(\frac{3-s}{n-s} \right)^3 (t + t_{\text{int}})^{\alpha_i} \theta(t_{\text{RS},*} - t), \quad (20)$$

where $\theta(t_{\text{RS},*} - t)$ and $\theta(t_{\text{FS,BO}} - t)$ represent the Heaviside step function controlling the end times of the FS and RS, respectively. $t_{\text{int}} \approx R_{\text{in}}/v_{\text{SN}}$ is the time when the ejecta just touches the CSM, representing the beginning of the ejecta–CSM interaction. The temporal index is $\alpha_i = (2n + 6s - ns - 15)/(n - s)$. Here, we fix $n = 7$ and $s = 0$, such that one has $\alpha_i = -0.143$.

The RS termination timescale $t_{\text{RS},*}$ is defined as the time for the RS to sweep up all of the effective ejecta (Chatzopoulos et al. 2012, 2013):

$$t_{\text{RS},*} = \left[\frac{v_{\text{KN}}}{\beta_{\text{RS}} (Ag_n/q)^{\frac{1}{n-s}}} \left(1 - \frac{(3-n)M_{\text{ej}}}{4\pi v_{\text{KN}}^{3-n} g_n} \right)^{\frac{1}{3-n}} \right]^{\frac{n-s}{s-3}} \quad (21)$$

where v_{KN} is the velocity of the kilonova ejecta. This depends on both the ejecta mass and the energy of the kilonova. Initially, we set v_{KN} as in the range of $0.1c$ to $0.9c$, and find that the apparent magnitude of the kilonova is affected a little bit by altering v_{KN} . So, we fixed v_{KN} as $0.1c$. The termination timescale of the FS is approximately equal to the time of the FS breakout $t_{\text{FS,BO}}$ when the optically thin⁵ part of the CSM is swept up, and is given as (Chatzopoulos et al. 2012, 2013)

$$t_{\text{FS,BO}} = \left\{ \frac{(3-s)q^{(3-n)/(n-s)} [Ag_n]^{(s-3)/(n-s)}}{4\pi\beta_{\text{FS}}^{3-s}} \right\}^{\frac{n-s}{(n-3)(3-s)}} \times M_{\text{CSM,th}}^{\frac{n-s}{(n-3)(3-s)}} \quad (22)$$

⁵ Here, the ‘‘optically thin’’ means that the optical depth is in the range of $2/3 < \tau_{\text{CSM}} < 1$.

where $M_{\text{CSM,th}}$ is the mass of the optically thin CSM:

$$M_{\text{CSM,th}} = \int_{R_{\text{in}}}^{R_{\text{ph}}} 4\pi r^2 \rho_{\text{CSM}} dr. \quad (23)$$

Here, we fix $R_{\text{in}} = 10^{15}$ cm. R_{ph} represents the photosphere radius of the CSM shell. Under the Eddington approximation, it is located at an optical depth $\tau_{\text{CSM}} = 2/3$ (Liu et al. 2018). R_{ph} is given by solving

$$\tau_{\text{CSM}} = \int_{R_{\text{ph}}}^{R_{\text{out}}} \kappa_{\text{CSM}} \rho_{\text{CSM}} dr = 2/3, \quad (24)$$

where κ_{CSM} is the optical opacity of the CSM and R_{out} is the radius of the outer boundary of the CSM. The opacities of the CSM shells and winds κ_{CSM} are related to their composition and temperatures. For hydrogen-poor matter, the dominant source of opacity is electron scattering, $\kappa_{\text{CSM}} = 0.06 - 0.2 \text{ cm}^2 \text{ g}^{-1}$ (see the references listed in Wang et al. 2016). For hydrogen-rich matter, $\kappa_{\text{CSM}} = 0.33 \text{ cm}^2 \text{ g}^{-1}$, which is the Thomson electron scattering opacity for fully ionized material with the solar metallicity (Chatzopoulos et al. 2012). It is given by solving

$$M_{\text{CSM}} = \int_{R_{\text{in}}}^{R_{\text{out}}} 4\pi r^2 \rho_{\text{CSM}} dr. \quad (25)$$

The total optical depth of the CSM depends on the opacity κ_{CSM} instead of M_{CSM} . For a given $M_{\text{CSM}} = 10M_{\odot}$ and hydrogen-rich matter $\kappa_{\text{CSM}} = 0.33 \text{ cm}^2 \text{ g}^{-1}$, the total optical depth of the τ_{CSM} is always larger than 1. If this is the case, one can only observe the kilonova that is contributed from both the RS and FS of the ejecta–CSM interaction. The interacting material could be heated by both the FS and RS, and contribute to the input total luminosity. One has

$$L_{\text{inp,CSM}}(t) = \epsilon [L_{\text{FS}}(t) + L_{\text{RS}}(t)], \quad (26)$$

where ϵ is the conversion efficiency from kinetic energy to radiation and is fixed at $\epsilon = 0.9$ to do the calculations, due to poor understanding. On the other hand, the optical depth is very important for the kilonova emission. If $\tau_{\text{CSM}} < 2/3$, one can observe the kilonova emission that is contributed from the r -process, spindown, as well as the RS of the CSM, but not the contribution from the FS of the CSM. If $2/3 < \tau_{\text{CSM}} < 1$, one can observe the kilonova emission that is contributed from r -process, spindown, as well as both the RS and FS of the ejecta–CSM interaction. If $\tau_{\text{CSM}} > 1$, one can always observe the kilonova emission that is only contributed from the RS and FS of the CSM, but one cannot observe the contributions from r -process and spindown. In order to observe the kilonova emission that is contributed from r -process, spindown, as well as both the RS and FS of the CSM, we set the total optical depth of the CSM τ_{CSM} in the range of $2/3 < \tau_{\text{CSM}} < 1$ for $\kappa_{\text{CSM}} = 0.2 \text{ cm}^2 \text{ g}^{-1}$. So that $M_{\text{CSM,th}}$ represents the mass of the optical depth larger than $2/3$. If this is the case, the output luminosity can be written as

$$L(t) = \frac{1}{t_{\text{diff}}} \exp \left[-\frac{t}{t_{\text{diff}}} \right] \int_0^t \exp \left[\frac{t'}{t_{\text{diff}}} \right] L_{\text{inp,CSM}}(t') dt' \quad (27)$$

where t_{diff} is the diffusion timescale. The interaction diffusion timescale can be written as

$$t_{\text{diff}} = \frac{\kappa_{\text{CSM}} M_{\text{CSM,th}}}{\phi c R_{\text{ph}}}, \quad (28)$$

where $\phi = 4\pi^3/9 \simeq 13.8$ (Arnett 1982).

Based on the Equation(11) together with Equation(12), one has

$$T_{\text{CSM}} = \left(\frac{L(t)}{4\pi R_{\text{ph}}^2 \sigma_{\text{SB}}} \right)^{1/4} \quad (29)$$

and

$$F_{\nu}^{\text{CSM}} = \frac{2\pi h\nu^3 R_{\text{ph}}^2}{D_{\text{L}}^2 c^2} \frac{1}{\exp(h\nu/kT_{\text{CSM}}) - 1}. \quad (30)$$

The observed kilonova emission flux consists of F_{ν}^{ejcta} which contains contributions from the r -process nucleosynthesis, spindown energy, and F_{ν}^{CSM} from the ejecta–CSM interaction:

$$F_{\nu}^{\text{tot}} = F_{\nu}^{\text{ejcta}} + F_{\nu}^{\text{CSM}}. \quad (31)$$

One may then determine the monochromatic apparent magnitude of the kilonova emission (Yu et al. 2018):

$$M_{\nu} = -2.5 \log_{10} \frac{F_{\nu}^{\text{tot}}}{3631} \text{Jy}. \quad (32)$$

Figure 1 shows a numerical calculation of the kilonova emission in the r band by considering the sum of the r -process-powered (marked L_{ra}), the spin energy from a magnetar (marked L_{sd}), and the ejecta–CSM interaction (marked CSM). We find that the most significant contribution to the kilonova emission from the ejecta–CSM interaction is at late times.

3. OBSERVATIONS OF GRB 191019A

GRB 191019A triggered the BAT at 15:12:33 UT on 2019 October 19 (Simpson et al. 2019). The light curve shows a complex structure with many overlapping pulses (Figure 2) with duration $T_{90} = 64 \pm 4$ s in the energy range 15 – 350 keV (Krimm et al. 2019), and thus GRB 191019A is classified as a typical long-duration GRB. The X-ray Telescope (XRT) began observing the field 3900 s after the BAT trigger (D’Ai et al. 2019). Several optical telescopes made follow-up observations of the field, such as the Ultraviolet and Optical Telescope, the Nordic Optical Telescope (NOT), Gemini-South, and the Hubble Space Telescope (Levan et al. 2023). Spectroscopy obtained with the NOT and Gemini-South found a redshift $z = 0.248$ within an old galaxy based on several absorption lines, and its location was pinpointed within 100 pc projected from the nucleus of its host galaxy (Levan et al. 2023).

The lack of an associated supernova and the evidence of no star formation in the host galaxy suggest that a massive star collapse origin of the progenitor of GRB 191019A is disfavored, and that the progenitor is likely to have arisen either from the merger of compact objects in dynamically dense stellar clusters or in a gaseous disk around a supermassive BH (Levan et al. 2023). Lazzati et al. 2023 proposed that GRB 191019A originated from a compact binary merger,

with a prompt emission intrinsic duration of ~ 1.1 s, which is stretched in time by the interaction with a high-density $\sim 10^7 - 10^8 \text{ cm}^{-3}$ external medium.

4. POSSIBLE KILONOVA EMISSION ASSOCIATED WITH GRB 191019A

If the merger of two compact stars is indeed taking place in GRB 191019A in the disk of an active galactic nucleus (AGN), the contribution to the kilonova emission from the ejecta–CSM interaction cannot be ignored in such a dense external medium. In this section, we calculate the emission of the GRB 191019A kilonova by considering both the r -process-powered energy and the ejecta–CSM interaction ($L_{\text{ra}} + \text{CSM}$), or the sum of the r -process-powered energy, the spin energy from a magnetar, and the ejecta–CSM interaction ($L_{\text{ra}} + L_{\text{sd}} + \text{CSM}$).

Lazzati et al. (2023) showed that the number density of the external medium can be as high as $10^7 - 10^8 \text{ cm}^{-3}$. By assuming that the external medium is filled with protons, the volume density is $\rho = 1.7 \times 10^{-16} \text{ g cm}^{-3}$. We calculate the kilonova emission given the ejecta masses of $M_{\text{ej}} = 10^{-2}, 10^{-3}, 10^{-4}, 10^{-5}$, and $10^{-6} M_{\odot}$ by considering both $L_{\text{ra}} + \text{CSM}$ (the left panel in Figure 3) and $L_{\text{ra}} + L_{\text{sd}} + \text{CSM}$ (the right panel in Figure 3). We find that a larger ejecta mass has a stronger L_{ra} radiation, but a smaller ejecta mass corresponds to a brighter kilonova emission contribution from the ejecta–CSM interaction at later time. Moreover, we also show that how the sensitivity of the kilonova emission is for different values of ejecta velocity and CSM mass (Figure 4). We find that the CSM interaction contribution of the kilonova emission is not sensitive to the ejecta velocity, but depends a little bit on the CSM mass. Here, a large mass of CSM is possible due to external environmental influence (such as gas drag or migration traps).

One basic question is whether or not we can find evidence for a kilonova emission from an ejecta–CSM interaction from the observations. We collect all the optical data that was observed by telescopes in Levan et al. (2023) in the r , g , z , U , and B bands. We find that the host galaxy of GRB 191019A is brighter than any afterglow or kilonova emission, except in the U band at early times. Therefore, it would be difficult to detect any kilonova emission from GRB 191019A. If this is the case, one interesting question is: what is the parameter distribution for a nondetection of a kilonova emission from GRB 191019A? Figure 5 shows the possible kilonova emission, which is dimmer than the host galaxy and cannot be detected within the $L_{\text{ra}} + L_{\text{sd}} + \text{CSM}$ scenario. A nondetection requires that the injected mass is larger than $M_{\text{ej}} = 2 \times 10^{-4} M_{\odot}$ and the injected luminosity and magnetar timescale are less than $L_0 = 10^{48} \text{ erg s}^{-1}$ and $t_{\text{sd}} = 10^3$ s, respectively.

The other case is that if the host galaxy is not bright enough or the kilonova emission of GRB 191019A is brighter than the host galaxy. Figure 6 shows a possible kilonova emission which is brighter than the host galaxy and can be detected within the $L_{\text{ra}} + L_{\text{sd}} + \text{CSM}$ scenario. It requires that the injected mass is less than $M_{\text{ej}} = 2 \times 10^{-5} M_{\odot}$ and the injected luminosity and magnetar timescale to be larger than $L_0 = 10^{48} \text{ erg s}^{-1}$ and $t_{\text{sd}} = 10^3$ s, respectively. If this is the case, the component of the kilonova emission from the ejecta–CSM interaction can be embodied at the later time.

5. CONCLUSION AND DISCUSSION

The prompt emission light curve of GRB 191019A shows a complex structure with a duration of $T_{90} = 64 \pm 4$ s in the energy range 15 – 350 keV (Krimm et al. 2019), and the GRB is classified as a typical long-duration GRB. It is quite different from that of typical short GRBs and short GRBs with EE (e.g. GRBs 060614 and 211211A). However, the lack of an associated supernova at low redshift $z = 0.248$ and the evidence that it lives in a host galaxy with no star formation suggest that a massive star collapse origin of the progenitor of GRB 191019A is disfavored, and it likely originated in a compact object merger (Levan et al. 2023). Lazzati et al. (2023) proposed that it may form dynamically in dense stellar clusters or originate in a gaseous disk around the supermassive BH. If this is the case, the prompt emission of GRB 191019A can be easily interpreted as having a short intrinsic duration that was stretched in time by the interaction with a dense external medium and seen as moderately off-axis (Lazzati et al. 2022, 2023).

If GRB 191019A is indeed taking place in such high-density environment after a compact binary merger (NS-NS or NS-BH) on the AGN’s disk, then the contribution to the kilonova emission from an ejecta–CSM interaction cannot be ignored. In this paper, we theoretically calculate the kilonova emission by considering the contribution of the ejecta–CSM interaction in the high-density environment, the r -process-powered energy, as well as the magnetar spin energy. It is found that the significant contribution to the kilonova emission from the ejecta–CSM interaction occurs at the later time. In this case, a larger ejecta mass has a stronger L_{ra} radiation, but a smaller ejecta mass corresponds to a brighter kilonova emission contribution from the ejecta–CSM interaction at a later time. This work is distinct from previous works that have not considered the contribution from the ejecta–CSM interaction to the kilonova emission.

Moreover, we try to apply it to GRB 191019A, but we find that it is difficult to identify the possible kilonova emission from the observations, due to the contribution of the bright host galaxy. By assuming that the brightness of the host galaxy is at the upper limit of the kilonova emission associated with GRB 191019A, the model requires that the injected mass is larger than $M_{\text{ej}} = 2 \times 10^{-4} M_{\odot}$ and the injected luminosity and magnetar timescale are less than $L_0 = 10^{48}$ erg s $^{-1}$ and $t_{\text{sd}} = 10^3$ s, respectively. On the other hand, a detected associated kilonova emission to GRB 191019A would require the injected mass be less than $M_{\text{ej}} = 2 \times 10^{-5} M_{\odot}$ and the injected luminosity and magnetar timescale to be larger than $L_0 = 10^{48}$ erg s $^{-1}$ and $t_{\text{sd}} = 10^3$ s,

respectively. Those values of the parameters fall into a reasonable range (Fryer et al. 2015; Côté et al. 2017), and the component of the kilonova emission due to the ejecta–CSM interaction can be embodied at later times if the host galaxy is not bright enough.

Our calculations also pose a curious question: is the nondetection of an associated kilonova emission to GRB 191019A due to a larger optical depth that presents photons from escaping the system before the medium becomes transparent at the photosphere radius? Based on the parameters we use in Figure 5 and Figure 6, we calculate the optical depth of the ejecta–CSM interaction and find that the optical depth is close to or even less than 1. This implies that the nondetection of any associated kilonova emission from GRB 191019A is not due to a large optical depth, but is either overwhelmed by the bright contribution from the host galaxy or that the kilonova emission is itself weak.

In the future, in order to investigate the kilonova emission contribution from the ejecta–CSM interaction associated with a GRB 191019A–like event, a brighter kilonova emission (at least brighter than that of the host galaxy) or an even lower redshift will be required. There are event rate densities of NS-NS ($R_{\text{NS-NS}} \sim f_{\text{AGN}}[0.2, 400] \text{ Gpc}^{-3} \text{ yr}^{-1}$) and NS-BH ($R_{\text{NS-BH}} \sim f_{\text{AGN}}[10, 300] \text{ Gpc}^{-3} \text{ yr}^{-1}$) mergers in the disks of AGNs (McKernan et al. 2020; Zhu et al. 2021). They also suggested that only 10%-20% of NS-BH mergers in AGN disks can result in tidal disruptions. If this is the case, the expected a detection rate is $R_{\text{obs}} \sim f_{\text{AGN}} f_{\theta}[20, 400] \text{ yr}^{-1}$. Here, f_{θ} is the fraction of mergers and f_{AGN} is the fraction of the observed NS-NS or NS-BH mergers from an AGN disk. We therefore encourage optical follow-up observations of GRB 191019A–like events, especially those that capture electromagnetic signals at later times if the host galaxy is not bright enough. If possible, an observed GRB 191019A-like event with an associated GW signal would also provide a good probe for understanding the types of compact star mergers (e.g., NS-NS or NS-BH).

The James Webb Space Telescope (JWST) has a near-infrared limit of 28. If the contribution of the host galaxy is very small, current detectors would be able to see such kilonova emission in the future.

We thank Bing Zhang and Ren Jia for helpful comments. This work is supported by the Guangxi Science Foundation the National (grant Nos. 2023GXNSFDA026007), the National Natural Science Foundation of China (grant No. 11922301 and 12133003), and the Program of Bagui Scholars Program (LHJ).

REFERENCES

- Abbott, B. P., Abbott, R., Abbott, T. D., et al. 2017, Phys. Rev. Lett., 119, 161101. doi:10.1103/PhysRevLett.119.161101
- Arnett, W. D. 1982, ApJ, 253, 785. doi:10.1086/159681
- Bellovary, J. M., Mac Low, M.-M., McKernan, B., et al. 2016, ApJ, 819, L17. doi:10.3847/2041-8205/819/2/L17
- Berger, E. 2011, NewAR, 55, 1. doi:10.1016/j.newar.2010.10.001
- Berger, E., Fong, W., & Chornock, R. 2013, ApJ, 774, L23. doi:10.1088/2041-8205/774/2/L23
- Berger, E. 2014, ARA&A, 52, 43. doi:10.1146/annurev-astro-081913-035926
- Chang, X.-Z., Lü, H.-J., Yang, X., et al. 2023, ApJ, 943, 146. doi:10.3847/1538-4357/aca969
- Chatzopoulos, E., Wheeler, J. C., & Vinko, J. 2012, ApJ, 746, 121. doi:10.1088/0004-637X/746/2/121
- Chatzopoulos, E., Wheeler, J. C., Vinko, J., et al. 2013, ApJ, 773, 76. doi:10.1088/0004-637X/773/1/76
- Chatzopoulos, E., Wheeler, J. C., & Vinko, J. 2012, ApJ, 746, 121. doi:10.1088/0004-637X/746/2/121
- Chevalier, R. A. & Fransson, C. 1994, ApJ, 420, 268. doi:10.1086/173557
- Chevalier, R. A. & Irwin, C. M. 2011, ApJ, 729, L6. doi:10.1088/2041-8205/729/1/L6

- Chevalier, R. A. 1982, *ApJ*, 258, 790. doi:10.1086/160126
- Covino, S., Wiersema, K., Fan, Y. Z., et al. 2017, *Nature Astronomy*, 1, 791
- Côté, B., Belczynski, K., Fryer, C. L., et al. 2017, *ApJ*, 836, 230. doi:10.3847/1538-4357/aa5c8d
- Dai, Z. G., & Lu, T. 1998, *Physical Review Letters*, 81, 4301
- Dai, Z. G., Wang, X. Y., Wu, X. F., et al. 2006, *Science*, 311, 1127. doi:10.1126/science.1123606
- D’Ai, A., Melandri, A., D’Avanzo, P., et al. 2019, *GCN*, 26045, 1
- Della Valle, M., Chincarini, G., Panagia, N., et al. 2006, *Nature*, 444, 1050. doi:10.1038/nature05374
- Eichler, D., Livio, M., Piran, T., et al. 1989, *Nature*, 340, 126. doi:10.1038/340126a0
- Evans, P. A., Cenko, S. B., Kennea, J. A., et al. 2017, *Science*, 358, 1565. doi:10.1126/science.aap9580
- Ferro, M., Brivio, R., D’Avanzo, P., et al. 2023, *A&A*, 678, A142. doi:10.1051/0004-6361/202347113
- Fynbo, J. P. U., Watson, D., Thöne, C. C., et al. 2006, *Nature*, 444, 1047. doi:10.1038/nature05375
- Fryer, C. L., Belczynski, K., Ramirez-Ruiz, E., et al. 2015, *ApJ*, 812, 24. doi:10.1088/0004-637X/812/1/24
- Gal-Yam, A., Fox, D. B., Price, P. A., et al. 2006, *Nature*, 444, 1053. doi:10.1038/nature05373
- Gao, H., Ding, X., Wu, X.-F., et al. 2015, *ApJ*, 807, 163. doi:10.1088/0004-637X/807/2/163
- Gao, H., Zhang, B., Lü, H.-J., et al. 2017, *ApJ*, 837, 50. doi:10.3847/1538-4357/aa5be3
- Gehrels, N., Norris, J. P., Barthelmy, S. D., et al. 2006, *Nature*, 444, 1044. doi:10.1038/nature05376
- Goldstein, A., Veres, P., Burns, E., et al. 2017, *ApJ*, 848, L14
- Gompertz, B. P., Rasio, M. E., Nicholl, M., et al. 2023, *Nature Astronomy*, 7, 67. doi:10.1038/s41550-022-01819-4
- Hotokezaka, K., Kiuchi, K., Kyutoku, K., et al. 2013, *Phys. Rev. D*, 87, 024001. doi:10.1103/PhysRevD.87.024001
- Jin, Z.-P., Li, X., Cano, Z., et al. 2015, *ApJ*, 811, L22. doi:10.1088/2041-8205/811/2/L22
- Jin, Z.-P., Hotokezaka, K., Li, X., et al. 2016, *Nature Communications*, 7, 12898. doi:10.1038/ncomms12898
- Jin, Z.-P., Covino, S., Liao, N.-H., et al. 2020, *Nature Astronomy*, 4, 77. doi:10.1038/s41550-019-0892-y
- Kasen, D. & Bildsten, L. 2010, *ApJ*, 717, 245. doi:10.1088/0004-637X/717/1/245
- Kasen, D., Metzger, B., Barnes, J., et al. 2017, *Nature*, 551, 80
- Korobkin, O., Rosswog, S., Arcones, A., et al. 2012, *MNRAS*, 426, 1940. doi:10.1111/j.1365-2966.2012.21859.x
- Kotera, K., Phinney, E. S., & Olinto, A. V. 2013, *MNRAS*, 432, 3228. doi:10.1093/mnras/stt680
- Kouveliotou, C., Meegan, C. A., Fishman, G. J., et al. 1993, *ApJ*, 413, L101. doi:10.1086/186969
- Krimm, H. A., Barthelmy, S. D., Cummings, J. R., et al. 2019, *GCN*, 26046, 1
- Lü, H.-J., Liang, E.-W., Zhang, B.-B., et al. 2010, *ApJ*, 725, 1965. doi:10.1088/0004-637X/725/2/1965
- Lü, H.-J., Zhang, B., Liang, E.-W., et al. 2014, *MNRAS*, 442, 1922. doi:10.1093/mnras/stu982
- Lü, H.-J., Zhang, H.-M., Zhong, S.-Q., et al. 2017, *ApJ*, 835, 181. doi:10.3847/1538-4357/835/2/181
- Lü, H.-J., Zou, L., Lan, L., et al. 2018, *MNRAS*, 480, 4402. doi:10.1093/mnras/sty2176
- Lü, H.-J., Yuan, Y., Lan, L., et al. 2020, *ApJ*, 898, L6. doi:10.3847/2041-8213/aba1ed
- Lü, H.-J., Yuan, H.-Y., Yi, T.-F., et al. 2022, *ApJ*, 931, L23. doi:10.3847/2041-8213/ac6e3a
- Lamb, G. P., Tanvir, N. R., Levan, A. J., et al. 2019, *ApJ*, 883, 48. doi:10.3847/1538-4357/ab38bb
- Lasky, P. D. & Glampedakis, K. 2016, *MNRAS*, 458, 1660. doi:10.1093/mnras/stw435
- Lazzati, D., Soares, G., & Perna, R. 2022, *ApJ*, 938, L18. doi:10.3847/2041-8213/ac98ad
- Lazzati, D., Perna, R., Gompertz, B. P., et al. 2023, *ApJ*, 950, L20. doi:10.3847/2041-8213/acd18c
- Levan, A. J., Malesani, D. B., Gompertz, B. P., et al. 2023, *Nature Astronomy*, 7, 976. doi:10.1038/s41550-023-01998-8
- Li, L.-X. & Paczyński, B. 1998, *ApJ*, 507, L59. doi:10.1086/311680
- Liu, L.-D., Wang, L.-J., Wang, S.-Q., et al. 2018, *ApJ*, 856, 59. doi:10.3847/1538-4357/aab157
- Ma, S.-B., Xie, W., Liao, B., et al. 2021, *ApJ*, 911, 97. doi:10.3847/1538-4357/abe71b
- Matzner, C. D. & McKee, C. F. 1999, *ApJ*, 510, 379. doi:10.1086/306571
- McKernan, B., Ford, K. E. S., & O’Shaughnessy, R. 2020, *MNRAS*, 498, 4088. doi:10.1093/mnras/staa2681
- Metzger, B. D. & Piro, A. L. 2014, *MNRAS*, 439, 3916. doi:10.1093/mnras/stu247
- Metzger, B. D., Martínez-Pinedo, G., Darbha, S., et al. 2010, *MNRAS*, 406, 2650. doi:10.1111/j.1365-2966.2010.16864.x
- Metzger, B. D. 2017, *Living Reviews in Relativity*, 20, 3. doi:10.1007/s41114-017-0006-z
- Metzger, B. D. 2019, *Living Reviews in Relativity*, 23, 1. doi:10.1007/s41114-019-0024-0
- Nicholl, M., Smartt, S. J., Jerkstrand, A., et al. 2014, *MNRAS*, 444, 2096. doi:10.1093/mnras/stu1579
- Paczynski, B. 1986, *ApJ*, 308, L43. doi:10.1086/184740
- Paczynski, B. 1991, *AcA*, 41, 257
- Qi, Y.-Q., Liu, T., Huang, B.-Q., et al. 2022, *ApJ*, 925, 43. doi:10.3847/1538-4357/ac3757
- Qin, Y., Liang, E.-W., Liang, Y.-F., et al. 2013, *ApJ*, 763, 15. doi:10.1088/0004-637X/763/1/15
- Rastinejad, J. C., Gompertz, B. P., Levan, A. J., et al. 2022, *Nature*, 612, 223. doi:10.1038/s41586-022-05390-w
- Ren, J., Chen, K., Wang, Y., et al. 2022, *ApJ*, 940, L44. doi:10.3847/2041-8213/aca025
- Rezzolla, L., Giacomazzo, B., Baiotti, L., et al. 2011, *ApJ*, 732, L6. doi:10.1088/2041-8205/732/1/L6
- Rosswog, S., Piran, T., & Nakar, E. 2013, *MNRAS*, 430, 2585. doi:10.1093/mnras/sts708
- Rowlinson, A., O’Brien, P. T., Tanvir, N. R., et al. 2010, *MNRAS*, 409, 531. doi:10.1111/j.1365-2966.2010.17354.x
- Savchenko, V., Ferrigno, C., Kuulkers, E., et al. 2017, *ApJ*, 848, L15
- Simpson, K. K., Barthelmy, S. D., Gropp, J. D., et al. 2019, *GCN*, 26031, 1
- Smith, N. & McCray, R. 2007, *ApJ*, 671, L17. doi:10.1086/524681
- Tagawa, H., Haiman, Z., & Kocsis, B. 2020, *ApJ*, 898, 25. doi:10.3847/1538-4357/ab9b8c
- Tanvir, N. R., Levan, A. J., Fruchter, A. S., et al. 2013, *Nature*, 500, 547. doi:10.1038/nature12505
- Troja, E., Castro-Tirado, A. J., Becerra González, J., et al. 2019, *MNRAS*, 489, 2104. doi:10.1093/mnras/stz2255
- doi:10.1093/mnras/stz2184
- Troja, E., Fryer, C. L., O’Connor, B., et al. 2022, *Nature*, 612, 228. doi:10.1038/s41586-022-05327-3
- Usov, V. V. 1992, *Nature*, 357, 472
- Wang, S. Q., Liu, L. D., Dai, Z. G., et al. 2016, *ApJ*, 828, 87. doi:10.3847/0004-637X/828/2/87
- Yang, B., Jin, Z.-P., Li, X., et al. 2015, *Nature Communications*, 6, 7323. doi:10.1038/ncomms8323
- Yang, J., Ai, S., Zhang, B.-B., et al. 2022, *Nature*, 612, 232. doi:10.1038/s41586-022-05403-8
- Yu, Y.-W., Zhang, B., & Gao, H. 2013, *ApJ*, 776, L40. doi:10.1088/2041-8205/776/2/L40
- Yu, Y.-W., Liu, L.-D., & Dai, Z.-G. 2018, *ApJ*, 861, 114. doi:10.3847/1538-4357/aac6e5
- Yuan, Y., Lü, H.-J., Yuan, H.-Y., et al. 2021, *ApJ*, 912, 14. doi:10.3847/1538-4357/abedb1
- Zhang, B. & Mészáros, P. 2001, *ApJ*, 552, L35. doi:10.1086/320255
- Zhang, B., Zhang, B.-B., Virgili, F. J., et al. 2009, *ApJ*, 703, 1696. doi:10.1088/0004-637X/703/2/1696
- Zhang, B. & Yan, H. 2011, *ApJ*, 726, 90. doi:10.1088/0004-637X/726/2/90
- Zhang, B.-B., Zhang, B., Sun, H., et al. 2018, *Nature Communications*, 9, 447. doi:10.1038/s41467-018-02847-3
- Zhang, B. 2013, *ApJ*, 763, L22. doi:10.1088/2041-8205/763/1/L22
- Zhang, B. 2018, *The Physics of Gamma-Ray Bursts by Bing Zhang*. ISBN: 978-1-139-22653-0. Cambridge University Press, 2018. doi:10.1017/9781139226530
- Zhu, J.-P., Zhang, B., Yu, Y.-W., et al. 2021, *ApJ*, 906, L11. doi:10.3847/2041-8213/abd412

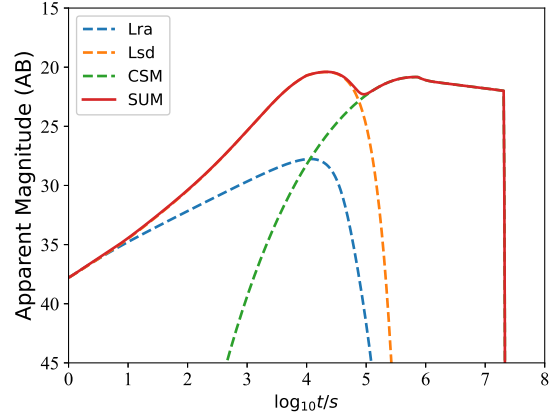


FIG. 1.— Kilonova r -band light curve considering the contributions from the three energy sources, e.g., the radioactive decay of heavier elements (the blue dashed line marked as L_{ra}), the magnetar spindown energy (the orange dashed line marked as L_{sd}) with typical values $M_{\text{ej}} = 10^{-4} M_{\odot}$, $\beta = v_{\text{KN}} = 0.1c$, $\kappa = 1.0 \text{ cm}^2 \text{ g}^{-1}$, $\tau = 10^4 \text{ s}$, and $L_0 = 1.0 \times 10^{47} \text{ erg s}^{-1}$, and the ejecta–CSM interaction (the green dashed line marked as CSM) with $E_{\text{KN}} = 10^{49} \text{ erg}$, $\kappa_{\text{CSM}} = 0.33 \text{ cm}^2 \text{ g}^{-1}$, $z = 0.248$, and $M_{\text{CSM}} = 10 M_{\odot}$. The red solid line is the sum of the three energy sources.

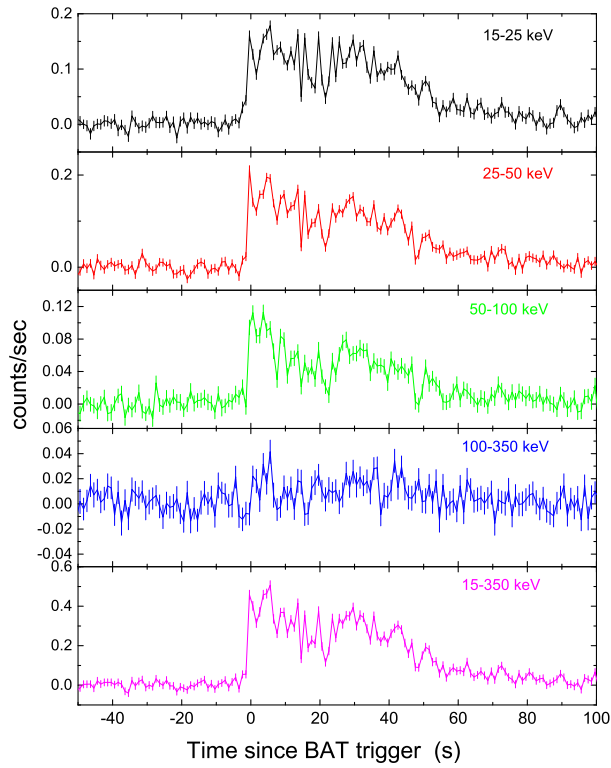


FIG. 2.— Swift/BAT light curves of GRB 191019A in different energy bands with a 256 ms time bin.

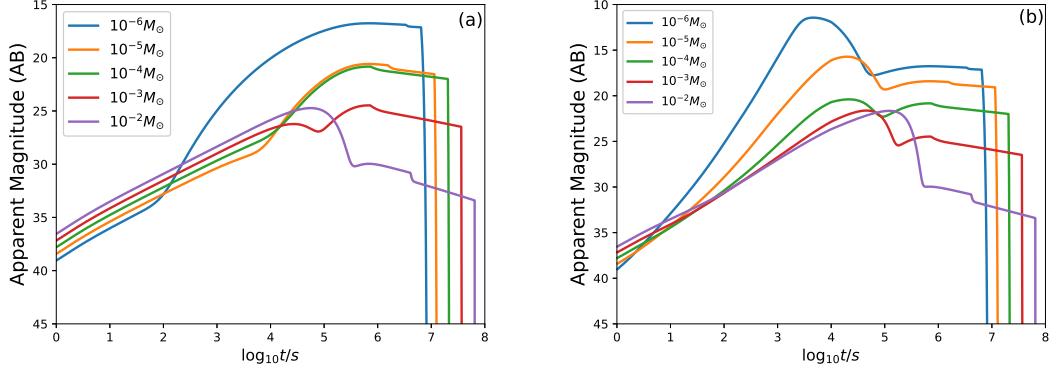


FIG. 3.— Kilonova r -band light curve with variations of $M_{\text{ej}} = 10^{-2}M_{\odot}$ (purple line), $10^{-3}M_{\odot}$ (red line), $10^{-4}M_{\odot}$ (green line), $10^{-5}M_{\odot}$ (orange line), and $10^{-6}M_{\odot}$ (blue line). (a) Considering the source energy of $L_{\text{ra}} + \text{CSM}$. (b) Considering the source energy of $L_{\text{ra}} + L_{\text{sd}} + \text{CSM}$. The other parameters are the same as in Figure 1.

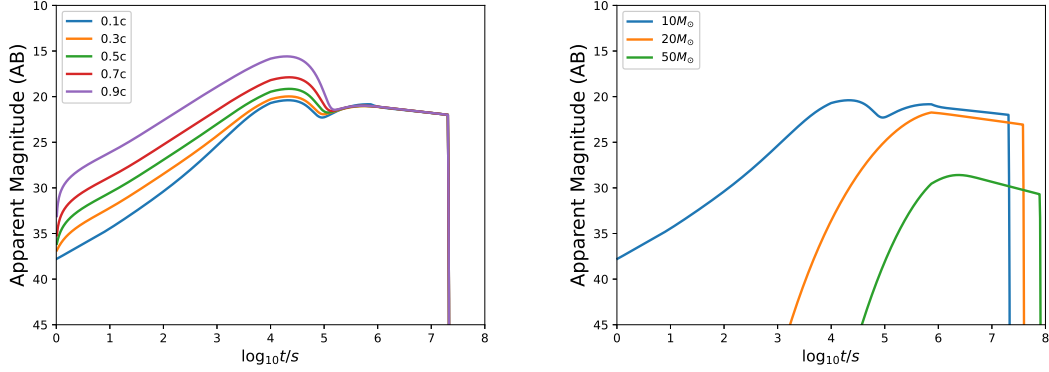


FIG. 4.— Kilonova r -band light curve with variations of ejecta velocity (left) and CSM mass (right). The other parameters are the same as in Figure 1.

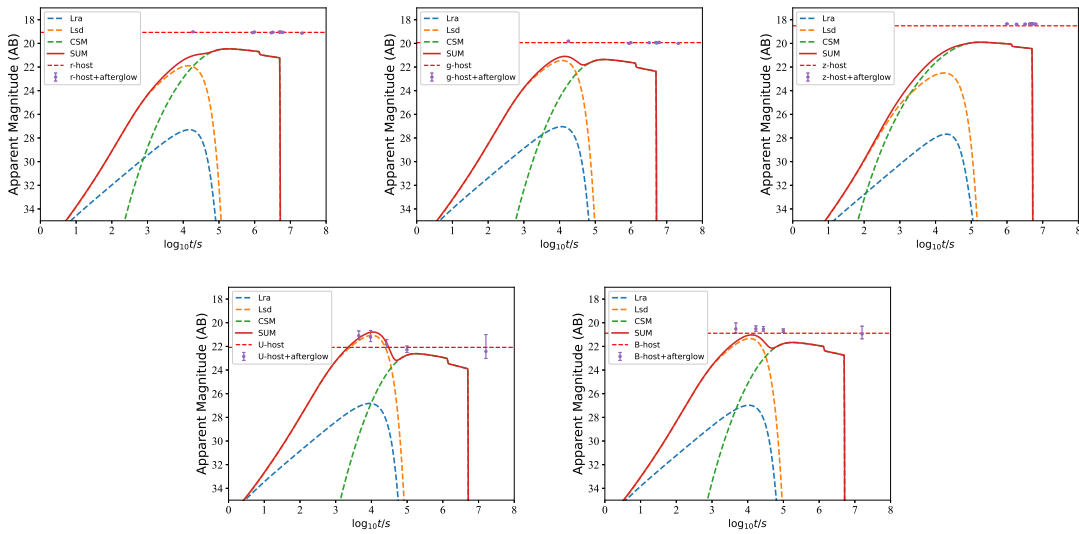


FIG. 5.— Kilonova light curves in the r , g , z , U , and B bands of GRB 191019A, considering the three energy sources. A kilonova nondetection requires $M_{\text{ej}} = 2 \times 10^{-4}M_{\odot}$, $\tau = 10^3$ s, and $L_0 = 10^{48}$ erg s^{-1} , $\kappa_{\text{CSM}} = 0.2 \text{ cm}^2 \text{ g}^{-1}$, and $E_{\text{KN}} = 3.5 \times 10^{49}$ erg. The red dashed line is the brightness of the host galaxy. The purple data points are the observations of host+afterglow collected from [Levan et al. \(2023\)](#).

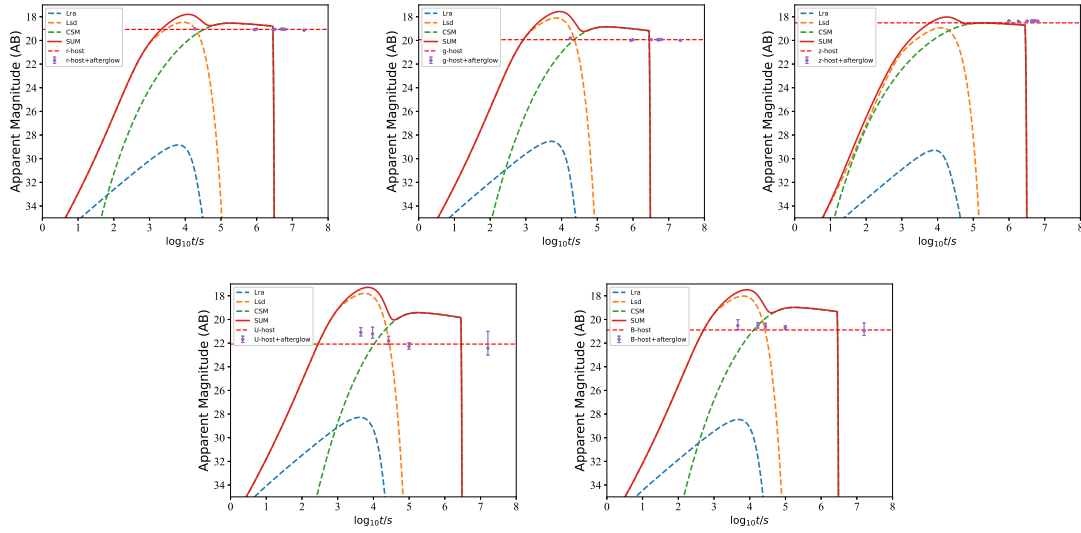


FIG. 6.— Kilonova light curves that are similar to Figure 5, but with a detected kilonova emission with the value of the parameter $M_{\text{ej}} = 2 \times 10^{-5} M_{\odot}$.